ISSN 1070-3632, Russian Journal of General Chemistry, 2008, Vol. 78, No. 4, pp. 723–731. © Pleiades Publishing, Ltd., 2008.
Published in Rossiiskii Khimicheskii Zhurnal, 2007, Vol. 51, No. 5, pp. 49–55.

Mechanistic Possibilities for Oxetane Formation in the Biosynthesis of Taxol's D Ring

Dan Willenbring and Dean J. Tantillo

University of California—Davis, Department of Chemistry,
One Shields Avenue, Davis, California, 95616
e-mail: tantillo@chem.ucdavis.edu

Received February 27, 2007

Abstract—Three mechanistic possibilities for the formation of the oxetane (D ring) of Taxol were examined at various levels of theory [B3LYP/6-31+G(d,p), mPW1PW91/6-31+G(d,p), and MP2/6-31+G(d,p)] including one mechanism involving an unusual oxabicyclobutonium ion intermediate. The mechanisms examined differ considerably in terms of their predicted inherent activation barriers, and the requirements for acceleration of each by an enzyme active site are outlined. Our calculations provide an important starting point for future studies in this area. Also examined were previously published calculations on simple oxabicyclobutonium ions, as well as the all-carbon analog of the pathway involving the oxabicyclobutonium ion.

DOI: 10.1134/S1070363208040336

INTRODUCTION

Since the first reports over 40 years ago [1], Taxol has achieved vast popularity among researchers due to its unusual structure and its success as a therapeutic agent for fighting various cancers. Given the enormity of the research on this molecule concerning its structure [2], biosynthesis [3], laboratory synthesis [4–6], industrial supply [7, 8], and biological activity [9], it is perhaps surprising that this drug still holds on to a number of secrets.

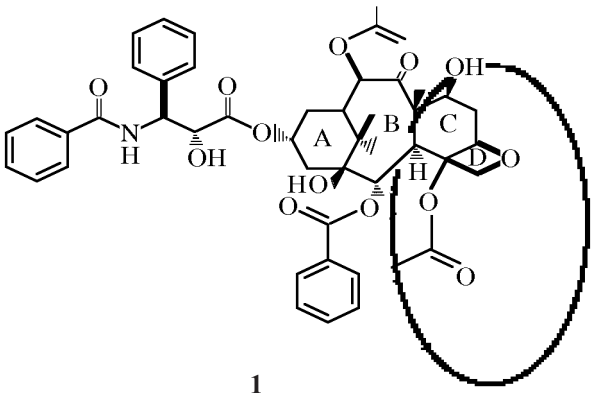

1

Of particular interest to us is the biosynthesis of the D ring of Taxol (**1**). While this oxetane ring, or a very close analog, is recognized as a necessary feature for microtubule binding in structure-activity studies [10], the enzyme that catalyzes its formation in Nature remains a mystery and its construction in the laboratory often provides a challenging hurdle for synthetic chemists [11]. Several groups have made chemically sound mechanistic proposals for the biosynthesis of the oxetanyl ester substructure [12–14] but the literature remains light on calculations that address the feasibility of such proposals [15]. We hope that the theoretical investigation described herein will provide a useful resource for further studies (both theoretical and experimental) on this subject.

METHODS

The structures reported herein (images generated with Ball & Stick 4.0a12 [16]) were optimized in the gas phase using the Gaussian 03 suite of programs [17] utilizing either the Becke three-parameter hybrid functional combined with the Lee–Yang–Parr correlation functional [18–21], second-order Møller–Plesset perturbation theory [22], or the Barone and Adamo one parameter functional using modified Perdew–Wang exchange and Perdew–Wang 91

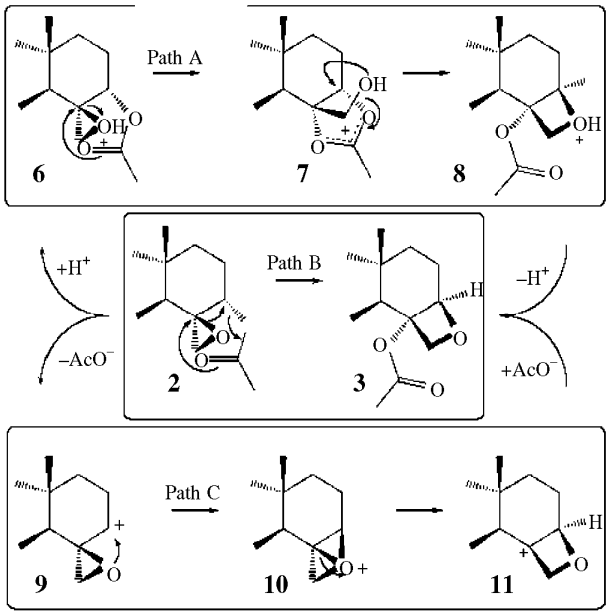

Fig. 1. Three investigated mechanistic pathways of oxetane ring formation. Path A: neutral, concerted, path B: stepwise, acid-catalyzed, and path C: dissociative.

correlation [23]. The 6-31+G(d,p) basis set was used in each case. These levels of theory are referred to throughout as B3LYP/6-31+G(d,p), MP2/6-31+G(d,p), and mPW1PW91/6-31+G(d,p), respectively. Hartree-Fock with the 6-31G(d) basis set [24] [referred to throughout as HF/6-31G(d)] was used to reproduce geometries from Swindell and Francl (*vide infra*) [15]. Structures labeled with a single number, **X**, are minima and structures labeled with two numbers, **TSXtoY**, are first-order saddle points (i.e. transition state structures) connecting minima **X** and **Y**. When animations associated with imaginary frequencies, from vibrational frequency analysis on stationary points, were ambiguous, saddle points were connected to minima using intrinsic reaction coordinate [25, 26] searches (see Supporting Information for details). Energy values reported are in kcal mol^{-1} and include zero-point energy corrections (with no scaling factors applied) unless noted otherwise.

RESULTS AND DISCUSSION

Our study began by identifying mechanistic proposals in the literature that were suitable for study with quantum-chemical calculations. Figure 1 summarizes the three mechanistic possibilities we explored, all of which involve epoxy ester precursors. The model system used for our calculations includes the carbon framework of the C and D rings of Taxol with methyl groups added where the B ring connects to the C ring (highlighted in red for **1**).

Neutral Pathway (Path A)

The neutral epoxy ester (path A, Fig. 1, center) can undergo a one step (i.e. concerted) rearrangement from **2** to the desired product **3** (Fig. 2). The transition state structure **TS2to3**, with only a 0.10 Å difference in length between breaking (2.18 Å) and forming (2.28 Å) C–O bonds of the migrating oxygen, and a 0.13 Å difference in length between breaking (1.74 Å) and forming (1.61 Å) C–O bonds of the migrating ester corresponds to a rearrangement that is synchronous as well as concerted. The magnitude of the barrier for this rearrangement, 48.3 kcal mol^{-1}, is not surprising considering the nature of the gas-phase calculations and the significant charge separation in the transition state structure, which can be thought of as containing alkoxide and dioxacarbenium substructures. The electrostatic potential surfaces in Fig. 2 nicely illustrate this point; there is clearly more separation of charge in the transition state **TS2to3** than either reactant **2** or product **3**. One can imagine that if an enzyme were to utilize this mechanism, it would need to selectively stabilize this distribution of charge in order to significantly lower the barrier [27].

This reaction is similar to the dyotropic rearrangements described by Reetz [27] in that two groups migrate past each other in a concerted process. However, in this case, one of the groups (the acetate unit) utilizes different atoms to bond to the carbon framework in the reactant and product and is therefore more like a hybrid of [1,2] and [2,3] sigmatropic shifts rather than of two [1,*n*] shifts.

Attempts to find a zwitterionic dioxacarbenium/alkoxide intermediate **4** (Fig. 3)—the sort of intermediate that might be expected for a stepwise rearrangement of the neutral system—were unsuccessful; starting geometries consistently rearranged to **2**, **3**, or ortho ester **5** during the geometry optimization procedure. Ortho ester **5** is 3.4 kcal mol^{-1} higher in energy than **2**, making it essentially energetically equivalent to **3**. One might envision an enzyme active site involved in catalyzing mechanism A that could discourage formation of the *ortho* ester product by exploiting the different geometric requirements to go from **2** to either **3** or **5** [28].

Giner and Faraldos [28] have investigated the possibility that ortho esters (like **5**), epoxy esters (like

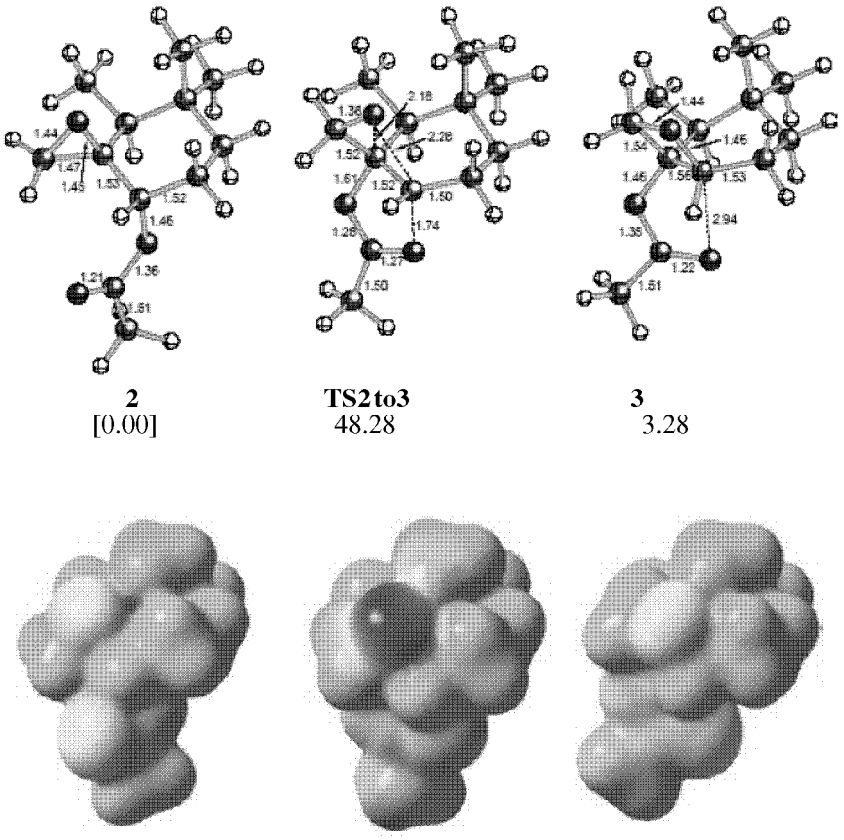

Fig. 2. (Top) B3LYP/6-31+G(d,p) geometries of neutral epoxy ester **2** rearranging to oxetanyl ester **3** through the transition state structure **TS2to3** [reaction path (a)]. (Bottom) Electrostatic potential surfaces for roughly the same orientation. Distances are reported in Å and energies in kcal mol^{-1} relative to **2**.

2), and oxetanyl esters (like **3**) in Taxol and related structures might function as latent electrophiles in biological systems. They suggest that these strained and reactive functional groups could, under biological conditions, rearrange and react with proteins in order to form covalent ligand–enzyme bonds in situations unrelated to microtubule binding events. Microtubule binding of Taxol has been shown to be a non-covalent interaction [29].

Protonated Pathway (Path B)

Adding a proton to the mix converts the concerted rearrangement of path A to a stepwise one (path B; Fig. 1, top) by providing significant stabilization to **4**; the resultant dioxacarbenium ion intermediate **7** (Fig. 4) is the lowest energy structure that we located along path B. The essentially barrierless (computed barriers of –0.3 kcal mol^{-1} with zero-point energy correction (ZPC), and 0.1 kcal mol^{-1} without) conversion of **6** to **7** (Figs. 1 and 4) correlates with the small geometric difference between epoxonium ion 6 and the transition structure **TS6to7**; the breaking C–O bond elongates by a mere 0.05 Å (from 1.68 to 1.73 Å) and the oxygen of the ether moves only 0.19 Å closer

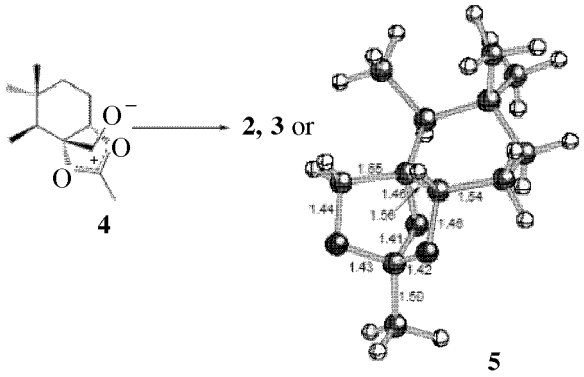

Fig. 3. Attempts to locate zwitterion **4** resulted in **2, 3** or ortho ester **5** (B3LYP/6-31+G(d,p) geometry shown with distances in Å).

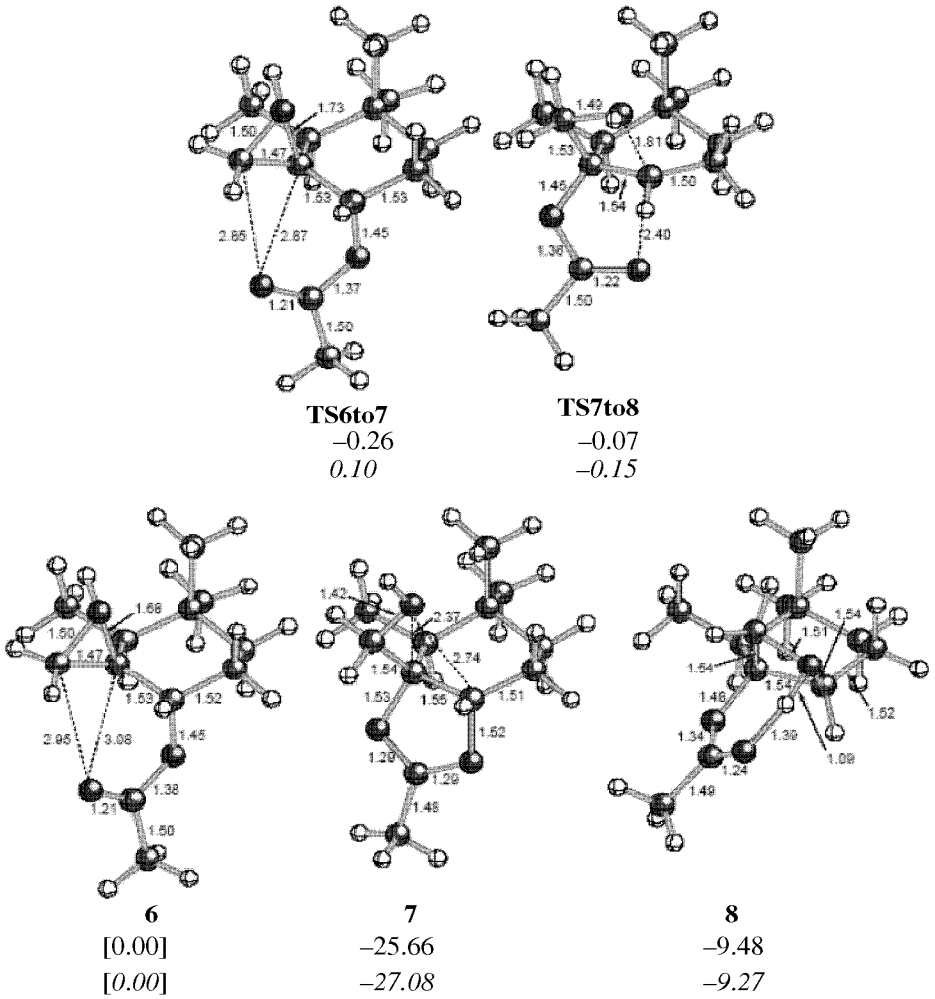

Fig. 4. B3LYP/6-31+G(d,p) geometries of epoxonim ion **6** rearranging to dioxacarbenium ion intermediate **7** through transition state structure **TS6to7**, and continuing to oxetanium ion **8** through the transition state structure **TS7to8**. Distances are reported in Å and energies in kcal mol^{-1} relative to **6**, (normal) with and (italics) without ZPC.

(from 3.06 Å to 2.87 Å) to the more electrophilic carbon of the epoxide. The small energetic and geometric changes associated with moving from 6 to **TS6to7** characterize **TS6to7** as a very early transition structure. Having the proton on the other face of the epoxide ring leads to analogous structures, which are trivially higher (on the order of half a kcal mol^{-1}) in energy (see Supporting information for details). Moving from **7** to **8** (Figs. 1 and 4) involves a significant barrier of 25.6 kcal mol^{-1} (26.9 kcal mol^{-1} without ZPC). With an enzyme to influence the reaction, such a barrier might be overcome, however, and likely byproducts stemming from intermediate **7** could be avoided.

One strategy for selectively stabilizing **TS7to8**, for example, would be to orient a hydrogen-bond donor near to the O of the breaking C–O bond. Interestingly, structure **8** includes an intramolecular hydrogen bond, which helps to stabilize the oxetanium ion product but not the transition state for its formation. A rotamer of **8** with the ester rotated to prevent such an interaction is 13.0 kcal mol^{-1} higher in energy than **8** so the energetics of such an interaction are almost certainly exaggerated by the nature of the gas-phase calculations.

Dissociative Pathway (Path C)

Path C, originally proposed by Swindell [12], involves an unusual oxabicyclobutonium ion inter-

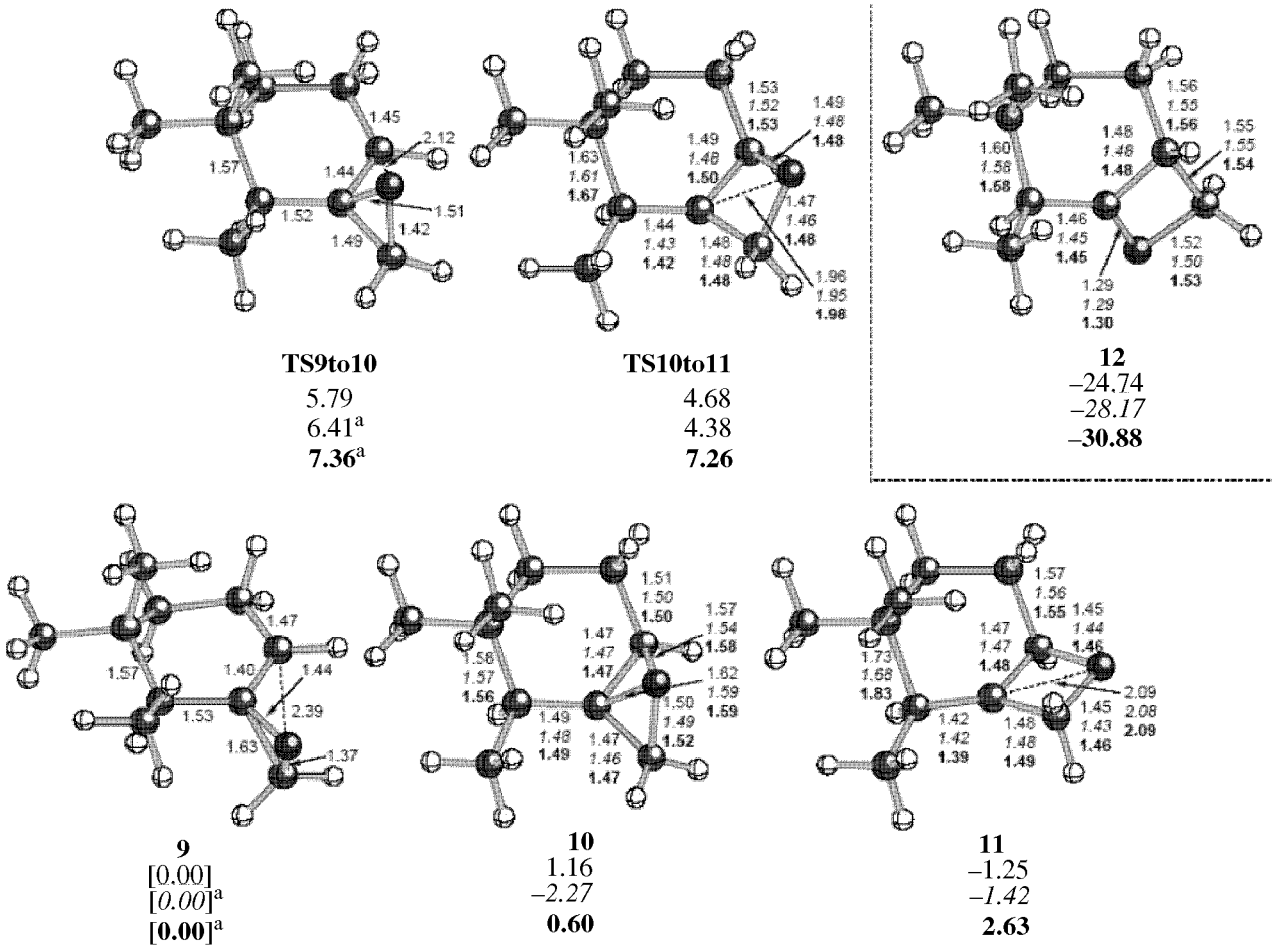

Fig. 5. B3LYP/6-31+G(d,p) geometries of **9** to **11** and **12** (path C). Distances are reported in Å and energies in kcal mol^{-1} relative to **9** at three levels of theory: (normal) B3LYP/6-31+G(d,p) with ZPC; (italics) mPW1PW91/6-31+G(d,p) with no ZPC; and (bold) MP2/6-31+G(d,p) with no ZPC. ([a]) Energies from single-point calculations at the respective level of theory using the B3LYP/6-31+G(d,p) geometry.

mediate **10** (Figs. 1 and 5). With such an unusual structure, we thought it prudent to examine this pathway with several levels of theory. While stationary points for **10**, **TS10to11,** and **11** were located at all three levels of theory used (B3LYP, mPW1PW91, and MP2, all with the 6-31+G(d,p) basis set), we were only able to locate **9** and **TS9to10** with B3LYP/6-31+G (d,p), despite vigorous efforts. All attempts using mPW1PW91 and MP2 to locate these structures resulted in **10** or **12** (an apparent dead-end as far as taxol biosynthesis is concerned) during the geometry optimization procedure (single point calculations using the B3LYP/6-31+G(d,p) geometry provide a reasonable estimate for the energetics of structures **9** and **TS9to10**, and such values are shown in Figure 4). It should be noted that Swindell found evidence for intermediates resembling **12** in an analogous system under some experimental conditions, and given that this structure is 24.8 kcal mol^{-1} lower in energy than **9**, this is no surprise. The computed energies and geometries match reasonably well across all three levels of theory. Moving from **9** to **10**, the barriers range from 5.8 kcal mol^{-1} [B3LYP/6-31+G(d,p)] to 7.4 kcal mol^{-1} [MP2/6-31+G(d,p) single point], and intermediate **10** is relatively close in energy to **9** in each case, ranging from –2.3 kcal mol^{-1} [mPW1PW91/6-31+G(d,p)] to 1.2 kcal mol^{-1} [B3LYP/6-31+G(d,p)]. The longest of the three C–O bonds in **10**, the one breaking in **TS10-to11**, ranges from 1.59 Å [mPW1PW91/6-31+G(d,p) and MP2/6-31+G(d,p)] to 1.62 Å [B3LYP/6-31+

G(d,p)], well within the range one might expect for a C–O bond in strained epoxonium ions [30]. The energies for **TS10to11** are 4.68 [B3LYP/6-31+G(d,p)], 4.38 [mPW1PW91/6-31+G(d,p)] and 7.26 [MP2/6-31+G(d,p)], slightly lower than the **TS9to10** energies in each case. The structure of **11** is most sensitive to the level of theory used. At the MP2 level, **11** shows much stronger hyperconjugation with the C–C bond of the cyclohexane ring versus the other two levels of theory, as this bond is elongated from 1.68 Å [mPW1PW91/6-31+G(d,p)] to 1.83 Å [MP2/6-31+G(d,p)]. The adjacent C–C^+ bond follows the same trend and while very similar at all three levels of theory, it is 0.03 Å shorter at MP2/6-31+G(d,p) versus both B3LYP/6-31+G(d,p) and mPW1PW91/6-31+G(d,p). In any case, **11** is primed for attack by a carboxylate ion leading to the taxol-like product. It is certainly possible that this carboxylate ion would be the same one that would have been initially lost to generate **9**. With no overwhelming barriers to contend with, there is no doubt that this type of rearrangement is feasible, though an enzyme may be needed to prevent competing rearrangements and other side reactions (through structures such as **12**, for example) [12].

Previous work from Francl and Swindell [15] provided experimental and theoretical support for rearrangements of the Path C type. Their model

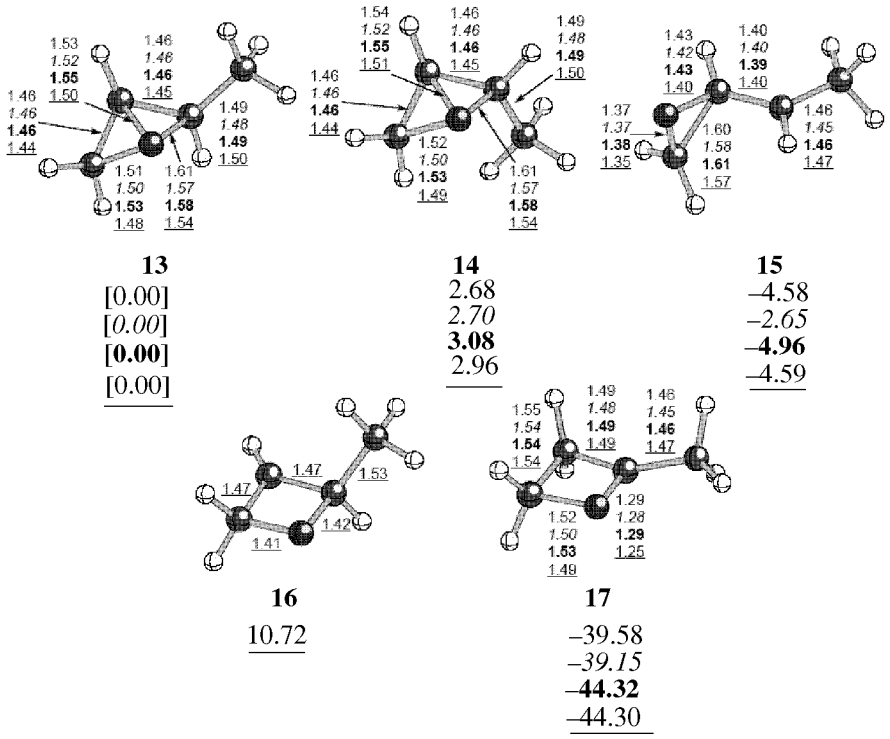

Fig. 6. B3LYP/6-31+G(d,p) geometries of **13** to **17** [31]. Distances are reported in Å and energies in kcal/mol with ZPC relative to **13** at four levels of theory: (normal) B3LYP/6-31+G(d,p); (italics) mPW1PW91/6-31+G(d,p); (bold) MP2/6-31+G(d,p); and (underlined) HF/6-31G(d). Structure **16** was only found at the HF level.

The following structure, a geometric isomer of those in Fig. 5, where the methyl group is on the center carbon shows expected elongation of the center C-O bond; the analogous structure for the Taxol rearrangement would be a combination between **13** and the one below:

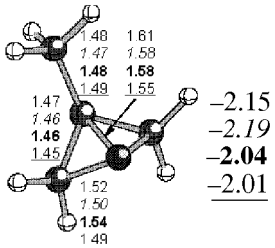

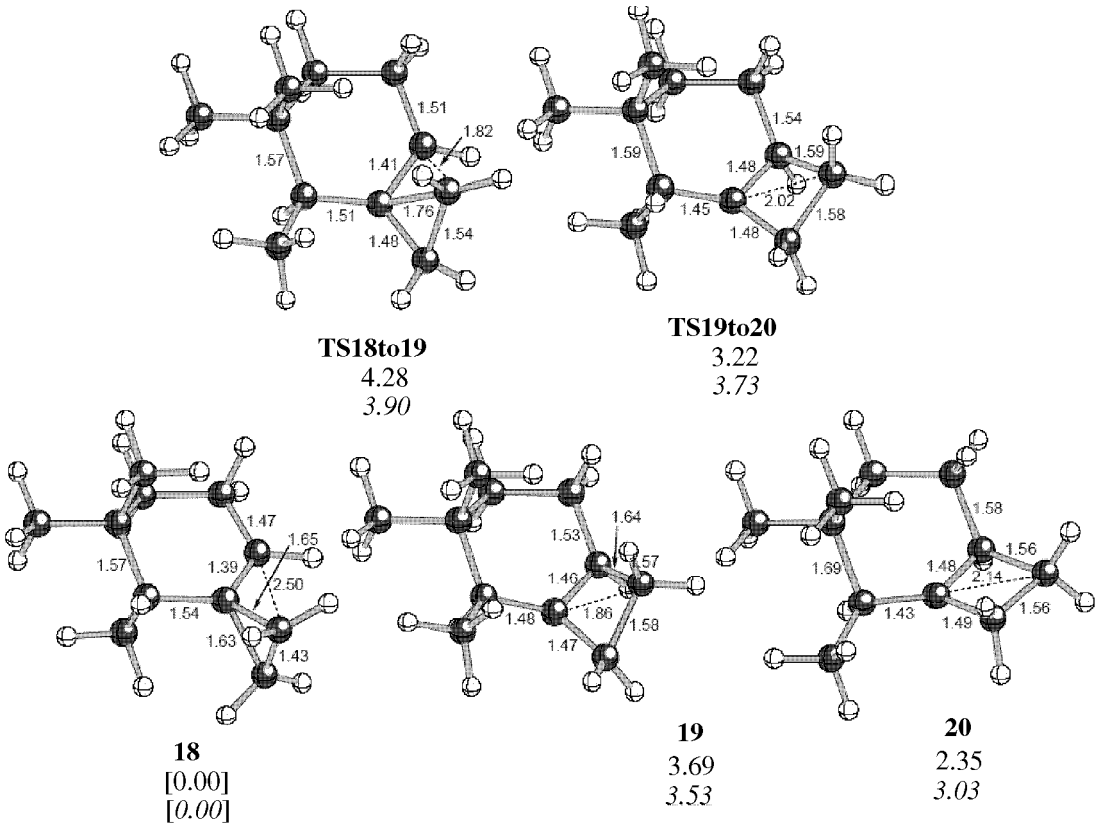

Fig. 7. B3LYP/6-31+G(d,p) geometries of **18** to **20** and transitions states **TS18to19** and **TS19to20**. Distances are reported in Å and energies in kcal mol^{-1} relative to **18** (normal) with and (italics) without ZPC.

system, structures **13–16** (Fig. 6), was originally optimized with HF/6-31G(d) and energies were determined from single-point calculations with MP2/6-31G(d). Our optimizations with higher levels of theory and larger basis sets resulted in similar geometries to those originally reported, with the exception of secondary cation **16**, which was only located with HF/6-31G(d). All attempts to locate **16** at other levels of theory resulted in **17** (the product of a 1,2-H shift) during the optimization procedure; this is not surprising, considering that **17** is >55 kcal mol^{-1} lower in energy than **16** at the HF/6-31G(d) level. While HF energies are consistent with those from higher levels of theory (probably a result of fortuitous cancellation of errors), the geometric differences are significant enough to affect single point energies computed at higher levels of theory.

We are particularly interested in the structures of unusual carbocations [31–36] and their relationships to heterosubstituted analogs, so we also calculated structures **18–20** (Fig. 7) of all-carbon analogs of **9**–**11**.

Starting with the α-cyclopropyl cation **18**, a fairly small barrier (4.3 kcal mol^{-1} with ZPC) leads to the non-classical bicyclobutonium ion **19**. The C–C bonds of the bicyclobutonium moiety, 1.58 Å, 1.64 Å, and 1.86 Å, range from long to very long, but clearly this structure contains a bridging methylene group (contrast with the classical cation **20**). An essentially barrierless drop from **19** to **20** liberates just over 1 kcal mol^{-1} (1.3 kcal mol^{-1} with ZPC). At this level of theory, the overall process is endothermic by 2.4 kcal mol^{-1} with ZPC. Although the same transformation with oxygen (Fig. 5) is overall slightly exothermic at the same level of theory and has slightly higher barriers, both transformations are comparable energetically.

CONCLUSIONS

While our gas-phase calculations do not distinguish which one of mechanisms A–C is more likely to predominate in the nature (since no enzyme that produces the D ring has yet been described), we have defined the inherent reactivity preferences that an

enzyme could enhance or overcome for such systems. For example, for path A to be followed, an enzyme will likely have to provide an environment that will significantly and selectively stabilize the charge distribution of **TS2to3.** We look forward to the discovery of an enzyme that catalyzes D ring formation so that the enzyme–substrate interactions that differentiate between the possible mechanisms can be elucidated. The calculations reported herein provide a starting point for such future studies.

REFERENCES

1. Wani, M.C., Taylor, H.L., Wall, M.E., Coggon, P., and McPhail, A.T., *J. Am. Chem. Soc.,* 1971, vol. 93, p. 2325.
2. Mastropaolo, D., Camerman, A., Luo, Y., Brayer, G.D., and Camerman, N., *Proc. Natl. Acad. Sci. USA*, 1995, vol. 92, p. 6920.
3. Croteau, R., Ketchum, R.E.B., Long, R.M., Kaspera, R., and Wildung, M.R., *Phytochem. Rev.* 2006, vol. 5, p. 75.
4. Holton, R.A., Somoza, C., Kim, H-B., Liang, F., Biediger, R.J., Boatman, P.D., Shindo, M., Smith, C.C., Kim, S., Nadizadeh, H., Suzuki, Y., Tao, C., Vu, P., Tang, S., Zhang, P., Murthi, K.K., Gentile, L.N., and Liu, J.H., *J. Am. Chem. Soc.*, 1994, vol. 116, p. 1597.
5. Holton, R.A., Kim, H-B., Somoza, C., Liang, F., Biediger, R.J., Boatman, P.D., Shindo, M., Smith, C. C., Kim, S., Nadizadeh, H., Suzuki, Y., Tao, C., Vu, P., Tang, S., Zhang, P., Murthi, K.K., Gentile, L.N., and Liu, J. H., *J. Am. Chem. Soc.*, 1994, vol. 116, p. 1599.
6. Nicolaou, K.C., Nantermet, P.G., Ueno, H., Guy, R.K., Couladouros, E.A., and Sorensen, E. J., *J. Am. Chem. Soc.*, 1995, vol. 117, p. 624.
7. Tabata, H., *Adv. Biochem. Engin. Biotechnol.*, 2004, vol. 7, p. 1.
8. Wuts, P.G.M., *Curr. Opin. Drug Disc. Devel.*, 1998, vol. 1, p. 329.
9. Schiff, P.B., Fant, J., and Horwitz, S.B., *Nature (London)*, 1979, vol. 277, p. 665.
10. Wang, M., Cornett, B., Nettles, J., Liotta, D.C., and Snyder, J.P., *J. Org. Chem.*, 2000, vol. 65, p. 1059.
11. Paquette, L.A. and Lo, H.Y., *J. Org. Chem.*, 2003, vol. 68, p. 2282.
12. Swindell, C.S. and Britcher, S.F., *J. Org. Chem.*, 1986, vol. 51, p. 793.
13. Guéritte-Voegelein, F., Guénard, D., and Potier, P., *J. Nat. Prod.*, 1987, vol. 50, p. 9.
14. Hefnerl, J., Rubenstein, S.M., Ketchum, R.E.B., Gibson, D.M., Williams, R.M., and Croteau, R., *Chem. Biol.*, 1996, vol. 3, p. 479.
15. Francl, M.M., Hansell, G., Patel, B. P., and Swindell, C.S., *J. Am. Chem. Soc.*, 1990, vol. 112, p. 3535.
16. Frisch, M.J., Trucks, G.W., Schlegel, H. B., Scuseria, G. E., Robb, M.A., Cheeseman, J.R., Montgomery, J.A., Jr., Vreven, T., Kudin, K.N., Burant, J. C., Millam, J.M., Iyengar, S.S., Tomasi, J., Barone, V., Mennucci, B., Cossi, M., Scalmani, G., Rega, N., Petersson, G.A., Nakatsuji, H., Hada, M., Ehara, M., Toyota, K., Fukuda, R., Hasegawa, J., Ishida, M., Nakajima, T., Honda, Y., Kitao, O., Nakai, H., Klene, M., Li, X., Knox, J.E., Hratchian, H. P., Cross, J. B.,Adamo, C., Jaramillo, J., Gomperts, R., Stratmann, R.E., Yazyev, O., Austin, A. J., Cammi, R., Pomelli, C., Ochterski, J. W., Ayala, P. Y., Morokuma, K., Voth, G.A., Salvador, P., Dannenberg, J.J., Zakrzewski, V.G., Dapprich, S., Daniels, A. D., Strain, M. C., Farkas, O., Malick, D.K., Rabuck, A.D., Raghavachari, K., Foresman, J.B., Ortiz, J.V., Cui, Q., Baboul, A.G., Clifford, S., Cioslowski, J., Stefanov, B.B., Liu, G., Liashenko, A., Piskorz, P., Komaromi, I., Martin, R.L., Fox, D.J., Keith, T., Al-Laham, M.A., Peng, C.Y., Nanayakkara, A., Challacombe, M., Gill, P.M.W., Johnson, B., Chen, W., Wong, M.W., Gonzalez, C., and Pople, J.A., *Gaussian 03*, Revision B.04, Pittsburgh PA: Gaussian, 2003**.**
17. Müller, N. and Falk, A., *Ball & Stick 4.0a12, Molecular Graphics Software for MacOS*, Linz: Johannes Kepler Univ., 2000.
18. Becke, A.D., *J. Chem. Phys*., 1993, vol. 98, p. 5648.
19. Stephens, P.J., Devlin, F.J., Chabalowski, C.F., and Frisch, M.J., *J. Phys. Chem*. 1994, vol. 98, p. 116237.
20. Lee, C., Yang, W., and Parr, R.G., *Phys. Rev. B*, 1988, vol. 37, p. 785.
21. Becke, A.D., *J. Chem. Phys*.б 1993, vol. 98, p. 1372.
22. Møller, C. and Plesset, M.S., *Phys. Rev*., 1934, vol. 4, p. 618.
23. Adamo, C. and Barone, V., *J. Chem. Phys.*, 1998, vol. 108, p. 664.
24. Hahriharan, P.C. and Pople, J.A., *Theor. Chim. Acta*, 1973, vol. 28, p. 213.
25. Gonzalez, C. and Schlegel, H. B., *J. Phys. Chem.*, 1990, vol. 94, p. 5523.
26. Fukui, K., *Acc. Chem. Res*., 1981, vol. 14, p. 363.
27. Reetz, M.T., *Angew. Chem., Int. Ed.*, 1972, vol. 11, p. 129; Reetz, M. T., *Ibid*., 1972, vol. 11, p. 130; Reetz, M.T., *Tetrahedron*, 1973, vol. 29, p. 2189; Reetz, M.T., *Adv. Organomet. Chem*., 1977, vol. 16, p. 33.
28. Giner, J.-L. and Faraldos, J.A., *Helv. Chim. Acta*, 2003, vol. 86, p. 3613.
29. Parness, J. and Horwitz, S.B., *J. Cell Biol.*, 1981, vol. 91, p. 479.
30. Zhao, Y. and Truhlar, D.G., *J. Org. Chem.*, 2007, vol. 72, p. 295.

31. Gutta, P. and Tantillo, D.J., *Org. Lett.*, 2007, vol. 9, p. 1069.
32. Siebert, M.R. and Tantillo, D.J., *J. Phys. Org. Chem*., in press.
33. Ponec, R., Bultinck, P., Gutta, P., and Tantillo, D. J., *J. Phys. Chem. A*, 2006, vol. 110, p. 3785.
34. Siebert, M.R. and Tantillo, D.J., *J. Org. Chem.*, 2006, vol. 71, p. 645.
35. Gutta, P. and Tantillo, D.J., *Angew. Chem. Int. Ed*., 2005, vol. 44, p. 2719.
36. Ponec, R., Yuzhakov, G., and Tantillo, D.J., *J. Org. Chem.,* 2004, vol. 69, p. 2992.